

# Evidence for a spin-aligned neutron-proton paired phase from the level structure of $^{92}\text{Pd}$

B. Cederwall<sup>b,1</sup> F. Ghazi Moradi,<sup>1</sup> T. Bäck,<sup>1</sup> A. Johnson,<sup>1</sup> J. Blomqvist,<sup>1</sup> E. Clément,<sup>2</sup>  
 G. de France,<sup>2</sup> R. Wadsworth,<sup>3</sup> K. Andgren,<sup>1</sup> K. Lagergren,<sup>1,4</sup> A. Dijon,<sup>2</sup>  
 G. Jaworski,<sup>5,6</sup> R. Liotta,<sup>1</sup> C. Qi,<sup>1</sup> B.M. Nyakó,<sup>7</sup> J. Nyberg,<sup>8</sup> M. Palacz,<sup>5</sup>  
 H. Al-Azri,<sup>3</sup> G. de Angelis,<sup>9</sup> A. Ataç,<sup>10</sup> S. Bhattacharyya<sup>c,2</sup> T. Brock,<sup>3</sup> J.R. Brown,<sup>3</sup>  
 P. Davies,<sup>3</sup> A. Di Nitto,<sup>11</sup> Zs. Dombrádi,<sup>7</sup> A. Gadea,<sup>12</sup> J. Gál,<sup>7</sup> B. Hadinia,<sup>1</sup>  
 F. Johnston-Theasby,<sup>3</sup> P. Joshi,<sup>3</sup> K. Juhász,<sup>13</sup> R. Julin,<sup>14</sup> A. Jungclaus,<sup>15</sup>  
 G. Kalinka,<sup>7</sup> S.O. Kara,<sup>10</sup> A. Khaplanov,<sup>1</sup> J. Kownacki,<sup>5</sup> G. La Rana,<sup>11</sup> S. M. Lenzi,<sup>16</sup>  
 J. Molnár,<sup>7</sup> R. Moro,<sup>11</sup> D. R. Napoli,<sup>9</sup> B. S. Nara Singh,<sup>3</sup> A. Persson,<sup>1</sup> F. Recchia,<sup>16</sup>  
 M. Sandzelius<sup>d,1</sup> J.-N. Scheurer,<sup>17</sup> G. Sletten,<sup>18</sup> D. Sohler,<sup>7</sup> P.-A. Söderström,<sup>8</sup>  
 M. J. Taylor,<sup>3</sup> J. Timár,<sup>7</sup> J. J. Valiente-Dobón,<sup>9</sup> E. Vardaci,<sup>11</sup> and S. Williams<sup>19</sup>

<sup>1</sup>*Department of Physics, Royal Institute of Technology, SE-10691 Stockholm, Sweden.*

<sup>2</sup>*Grand Accélérateur National d'Ions Lourds (GANIL),  
 CEA/DSM - CNRS/IN2P3, Bd Henri Becquerel,  
 BP 55027, F-14076 Caen Cedex 5, France.*

<sup>3</sup>*Department of Physics, University of York, YO10 5DD York, UK.*

<sup>4</sup>*Joint Institute for Heavy-Ion Research,  
 Holifield Radioactive Ion Beam Facility, Oak Ridge TN, 37831, USA.*

<sup>5</sup>*Heavy Ion Laboratory, University of Warsaw,  
 ul. Pasteura 5a, 02-093, Warsaw, Poland.*

<sup>6</sup>*Faculty of Physics, Warsaw University of Technology,  
 Koszykowa 75, 00-662, Warsaw, Poland.*

<sup>7</sup>*ATOMKI, H-4001 Debrecen, Hungary.*

<sup>8</sup>*Department of Physics and Astronomy,  
 Uppsala University, SE-75121 Uppsala, Sweden.*

<sup>9</sup>*Instituto Nazionale di Fisica Nucleare,  
 Laboratori Nazionali di Legnaro, I-35020 Legnaro, Italy.*

<sup>b</sup> Corresponding author: cederwall@nuclear.kth.se

<sup>c</sup> Present address: V.E.C.C, 1/AF Bidhan Nagar, Kolkata 700064, India.

<sup>d</sup> Present address: Department of Physics, University of Jyväskylä, FIN-40014 Jyväskylä, Finland.

<sup>10</sup>*Department of Physics, Ankara University, 06100 Tandogan Ankara, Turkey.*

<sup>11</sup>*Dipartimento di Scienze Fisiche, Università di Napoli and  
Istituto Nazionale di Fisica Nucleare, I-80126 Napoli, Italy.*

<sup>12</sup>*IFIC, CSIC, University of Valencia, Valencia, Spain.*

<sup>13</sup>*Department of Information Technology,  
University of Debrecen, H-4010 Debrecen, Hungary.*

<sup>14</sup>*Department of Physics, University of Jyväskylä, FIN-40014 Jyväskylä, Finland.*

<sup>15</sup>*Instituto de Estructura de la Materia, CSIC, E-28006 Madrid, Spain.*

<sup>16</sup>*Dipartimento di Fisica dell'Università di Padova and Istituto Nazionale di Fisica Nucleare,  
Sezione di Padova, I-35122 Padova, Italy.*

<sup>17</sup>*Université Bordeaux 1, CNRS/IN2P3,  
Centre d'Etudes Nucléaires de Bordeaux Gradignan, UMR 5797,  
Chemin du Solarium, BP120, 33175 Gradignan, France.*

<sup>18</sup>*The Niels Bohr Institute, University of Copenhagen, 2100 Copenhagen, Denmark.*

<sup>19</sup>*TRIUMF, Vancouver, BC, V6T 2A3, Canada.*

The general phenomenon of shell structure in atomic nuclei has been understood since the pioneering work of Goeppert-Mayer, Haxel, Jensen and Suess [1]. They realized that the experimental evidence for nuclear magic numbers could be explained by introducing a strong spin-orbit interaction in the nuclear shell model potential. However, our detailed knowledge of nuclear forces and the mechanisms governing the structure of nuclei, in particular far from stability, is still incomplete. In nuclei with equal neutron and proton numbers ( $N = Z$ ), the unique nature of the atomic nucleus as an object composed of two distinct types of fermions can be expressed as enhanced correlations arising between neutrons and protons occupying orbitals with the same quantum numbers. Such correlations have been predicted to favor a new type of nuclear superfluidity; isoscalar neutron-proton pairing [2–6], in addition to normal isovector pairing (see Fig. 1). Despite many experimental efforts these predictions have not been confirmed. Here, we report on the first observation of excited states in  $N = Z = 46$  nucleus  $^{92}\text{Pd}$ . Gamma rays emitted following the  $^{58}\text{Ni}(^{36}\text{Ar}, 2n)^{92}\text{Pd}$  fusion-evaporation reaction were identified using a combination of state-of-the-art high-resolution  $\gamma$ -ray, charged-particle and neutron detector systems. Our results reveal evidence for a spin-aligned, isoscalar neutron-proton coupling scheme, different from the previous prediction [2–6]. We suggest that this coupling scheme replaces normal superfluidity (characterized by seniority coupling [7, 8]) in the ground and low-lying excited states of the heaviest  $N = Z$  nuclei. The strong isoscalar neutron-proton correlations in these  $N = Z$  nuclei are predicted to have a considerable impact on their level structures, and to influence the dynamics of the stellar rapid proton capture nucleosynthesis process.

For all known nuclei, including those residing along the  $N = Z$  line up to around mass 80, a detailed analysis of their properties such as binding energies [9] and the spectroscopy of the excited states [10] strongly suggests that normal isovector ( $T = 1$ ) pairing is dominant at low excitation energies. On the other hand, there are long standing predictions for a change in the heavier  $N = Z$  nuclei from a nuclear superfluid dominated by isovector pairing to a structure where isoscalar ( $T = 0$ ) neutron-proton (np) pairing has a major influence as the mass number increases towards the exotic doubly magic nucleus  $^{100}\text{Sn}$  [2–6], the heaviest  $N = Z$  nucleus to be bound.

$N = Z$  nuclei with mass number  $> 90$  can only be produced in the laboratory with very low

cross sections and the associated problems of identifying the reaction products and their associated  $\gamma$  rays from the vast array of  $N > Z$  nuclei that are present in much greater numbers from the reactions used have prevented observation of their low-lying excited states until now. In the present work the experimental difficulties have been overcome through the use of a highly efficient, state-of-the-art detector system and a prolonged experimental running period.

Excited states in  $^{92}\text{Pd}$  were populated following heavy-ion fusion-evaporation reactions at the Grand Accélérateur National d'Ions Lourds (GANIL), France.  $^{36}\text{Ar}$  ions, accelerated to a kinetic energy of 111 MeV, were used to bombard an isotopically enriched (99.83%)  $^{58}\text{Ni}$  target. Light charged particles (mainly protons and alpha particles), neutrons and  $\gamma$  rays emitted in the reactions were detected in coincidence. A schematic layout of the experimental set-up is shown in Fig. 2.

The two-neutron (2n) evaporation reaction channel following formation of the  $^{94}\text{Pd}$  compound nucleus, leading to  $^{92}\text{Pd}$ , was very weakly populated with a relative yield of less than  $10^{-5}$  of the total fusion cross section. Gamma rays from decays of excited states in  $^{92}\text{Pd}$  were identified by comparing  $\gamma$ -ray spectra in coincidence with two emitted neutrons and no charged particles with  $\gamma$ -ray spectra in coincidence with other combinations of neutrons and charged particles. The typical efficiency for detecting any charged particle was 66%. This rises to 88% or higher if more than one such particle is emitted in the population of a particular exit channel. The clean identification of neutrons is crucial, since scattering of neutron events from one neutron detector segment to another can be misinterpreted as two neutrons, thereby giving rise to background from reaction channels where only one neutron has been emitted in  $\gamma$ -ray spectra gated by two neutrons. But, since neutrons have a finite velocity the difference in detection time is typically smaller for interactions resulting from two separate neutrons compared to a single scattered neutron. Background contributions from neutron scattering in 2n-gated spectra were significantly reduced by applying a criterion on the time difference in the time of flight parameter, relative to the distance between the neutron detectors firing. After such corrections the efficiency for correctly identifying both neutrons from a 2n-event was 3%. Figure 3 shows projected spectra from the charged particle-vetoed, 2n-selected  $E_{\gamma} - E_{\gamma}$  coincidence matrix when  $\gamma$  rays coincident with the 874 keV, 912 keV and 750 keV transitions (a), b), and c), respectively) assigned to  $^{92}\text{Pd}$  are selected. By comparing spectra with and without the charged particle veto condition applied it is clear that these  $\gamma$  rays are not associated with emission of charged particles from the compound nucleus. Fig. 3 d) shows a plot of the intensity ratios of the 874 keV, 912 keV and 750 keV  $\gamma$  rays in coincidence with two

neutrons and one neutron, respectively, proving that the  $\gamma$  rays assigned to  $^{92}\text{Pd}$  belong to the 2n-evaporation reaction channel. An extensive literature search was also performed in order to exclude the possibility that the  $\gamma$  rays assigned to  $^{92}\text{Pd}$  could be due to the decay of excited states in some other nucleus. In particular,  $\gamma$  rays from reactions involving possible target impurities were taken into account. See Supplementary Information for further details on the data analysis.

The three most intense  $\gamma$ -ray transitions assigned to  $^{92}\text{Pd}$  (874 keV, 912 keV and 750 keV) have been ordered into a ground state band based on their relative intensities (caption, Fig 3). Hence, the uncertainties in the relative intensities of the  $\gamma$ -ray transitions translates into a corresponding uncertainty in their ordering, and consequently, also in the absolute position of the  $4^+$  state. As shown in Fig 3, these  $\gamma$  rays form a mutually coincident decay sequence. Although the limited statistics precludes an accurate angular distribution analysis and hence firm spin assignments it is likely that the 874 keV, 912 keV and 750 keV  $\gamma$ -ray transitions constitute a cascade of stretched E2 transitions depopulating the first excited  $2^+$ ,  $4^+$ , and  $6^+$  states, respectively (Fig 3, right panel).

Nuclei immediately below  $^{100}\text{Sn}$  on the Segré chart, with  $Z, N < 50$ , may show special structural features since the active neutrons and protons here can move in many identical orbits. Here, for the heaviest  $N \approx Z$  nuclei, state-of-the-art shell model calculations predict ground-state and low-lying yrast structures based on spin-aligned systems of neutron-proton pairs to appear, similar to a scenario proposed by Danos and Gillet more than four decades ago [11]. The np-paired ground-state configuration emanates from the strong attractive interaction between  $g_{9=2}$  neutrons and protons in aligned angular momentum ( $J = 9$ ) coupling and is hence different from the predictions of a BCS type of isoscalar np pairing condensate in  $N \approx Z$  nuclei [2-6]. The shell model calculations were performed using empirical two-body matrix elements in the  $f_{5/2} p_{3/2} p_{1/2} g_{9/2}$  model space, see Supplementary Information for details. In Fig. 4 we show the results of our calculation as well as the corresponding experimental data resulting from the present work in  $^{92}\text{Pd}$  and from Refs. [12, 13] in  $^{94,96}\text{Pd}$ . The level structure of the semi-magic ( $N = 50$ ) nucleus  $^{96}\text{Pd}$ , with four proton holes relative to the  $Z = 50$  closed shell core, exhibits the typical traits of a nucleus in the normal isovector pairing phase for which the seniority coupling scheme dominates: A transition from the ground state to the first excited  $2^+$  state requires the breaking of one  $g_{9/2}$  proton-hole pair, and therefore the energy spacing between these two levels is rather large. The distance between the subsequent levels gradually decreases as the angular momentum vectors of the  $g_{9/2}$  quasiproton holes align until the  $8^+$  state is reached. Here, the angular momentum vectors of one pair of

proton holes are maximally aligned, and in order to reach higher-lying states the other pair has to be broken. This spin sequence terminates in the  $12^+$  state, where all four proton holes in the  $g_{9/2}$  orbital are fully aligned. In order to reach higher spin states, excitations must be made across the  $N, Z = 50$  shell gap, requiring much more energy. In contrast, the calculated spectrum of  $^{92}\text{Pd}$ , with four proton holes and four neutron holes relative to the  $^{100}\text{Sn}$  core, show a nearly constant energy spacing between consecutive levels. To examine the role played by the components of the np interaction in this spectrum we performed the same calculation while including only the  $T = 0$  component of the interaction matrix elements, including only the  $T = 1$  components, or excluding all np interactions (i. e. all  $T_z=0$  components). As seen in Fig. 4, the calculated spectrum of  $^{92}\text{Pd}$  for the latter case is very much like the spectrum of the closed neutron shell nucleus  $^{96}\text{Pd}$ . For the full calculation (case SM in Fig. 4) the calculated spectra agree very well with the experimental ones. It is evident that the  $T = 0$  component of the np interactions plays a dominating role for the spectrum of  $^{92}\text{Pd}$  while such interactions between the valence nucleons are absent in  $^{96}\text{Pd}$ . The calculated wave functions for the ground state and low-lying yrast states in  $^{92}\text{Pd}$  are completely dominated by the isoscalar np pairs in the spin-aligned  $J^\pi = 9^+$  coupling. The nucleus  $^{94}\text{Pd}$  represents an interesting intermediate case.

A simple semiclassical picture can help to illustrate why the yrast states in  $^{92}\text{Pd}$  are nearly equidistant, in terms of the overlap between the valence particle orbits. It is a consequence of the variation of the angle between the angular momentum vectors of np hole pairs circling in one direction and the angular momentum vectors of those circling in the opposite direction, as a function of the total angular momentum. This variation is approximately linear for small values of angular momentum. This mechanism for generating the total angular momentum in the nucleus is quite different from those present in normal superfluid nuclei. The regularly-spaced level sequence observed in the full calculation for  $^{92}\text{Pd}$  is therefore a distinct signature of the spin-aligned isoscalar mode, in the absence of collective vibrational excitations (see Supplementary Information for further details). The fact that the ordering of the experimentally observed  $\gamma$ -ray transitions is affected by some uncertainty does not change the interpretation of the data. The effect of a different ordering would be a maximal change in the  $2^+$  and  $4^+$  energies by 124 keV and 162 keV, respectively, in similar agreement with the theoretical prediction. The special topology of the ground-state wave function predicted for  $^{92}\text{Pd}$  is illustrated schematically in Fig. 4 (top left), and compared with the case for the normal pairing phase in  $^{96}\text{Pd}$  (top right). In the spin-aligned np

paired phase the main component of the nuclear ground-state wave function can, in a semiclassical picture, be regarded as built of a system of deuteron-like np hole pairs spinning around the core, each with maximum angular momentum. The special character of the wave function also implies a deformed intrinsic structure.

While the experimental data presented in this Letter strongly suggest that a spin-aligned neutron-proton paired phase is present in  $^{92}\text{Pd}$ , further experimental information is needed to confirm this interpretation. In particular measurements of particle transfer reactions,  $B(E2; 0^+ \rightarrow 2^+)$  values using Coulomb excitation, and precise mass measurements, would help to elucidate the structural evolution of nuclei along the  $N = Z$  line and to develop a better understanding of neutron-proton correlations and their implications for nuclear shell structure far from stability. This is also of importance for understanding reaction rates as well as the end point of the astrophysical rp-process [14, 15], which have impact on the composition and X-ray burst profiles of accreting neutron stars, and the nucleosynthesis of neutron deficient isotopes.

### Acknowledgements

This work was supported by the Swedish Research Council, the Göran Gustafsson Foundation, the European Union 6th Framework Programme “Integrating Infrastructure Initiative - Transnational Access”, No. 506065 (EURONS), the Hungarian Scientific Research Fund, OTKA, under Contract Nos. K72566 and K68801, the UK Engineering and Physical Sciences Research Programme “Interacting Infrastructure Initiative - Transnational Access”, the UK STFC, the Polish Ministry of Science and Higher Education grant No. N N202 073935, the Spanish Ministerio de Ciencia e Innovación under Contract No. FPA2007-66069, and Ankara University BIYEP project No. DPT 2005120140. The authors would like to thank the European Gamma-ray Spectroscopy Pool for use of the neutron detector system, L. Einarsson and R. Seppälä for providing some of the targets used in this experiment and the GANIL staff for technical support and for providing the  $^{36}\text{Ar}$  beam.

- 
- [1] Goeppert Mayer, M. On Closed Shells in Nuclei. II. Phys. Rev. **75**, 1969-1970 (1949).
  - [2] Goodman, A. L. Restoration of axial symmetry of the equilibrium shape of  $^{24}\text{Mg}$  by pairing correlations. Adv. Nucl. Phys. **11**, 260-263 (1979).

- [3] Engel, J., Langanke, K. & Vogel, P. Pairing and Isospin Symmetry in Proton-Rich Nuclei. Phys. Lett. **B389**, 211-216 (1966).
- [4] Engel, J. *et al.*. Neutron-proton correlations in an exactly solvable model. Phys. Rev. **C55**, 1781-1788 (1997).
- [5] Satula, W. & Wyss, R. Competition between  $T = 0$  and  $T = 1$  pairing in proton-rich nuclei. Phys. Lett. **B393**, 1-6 (1997).
- [6] Civitarese, O., Reboiro, M. & Vogel, P. Neutron-proton pairing in the BCS approach. Phys. Rev. **C56**, 1840-1843 (1997).
- [7] Talmi, I. Generalized seniority and structure of semi-magic nuclei. Nucl. Phys. **A172**, 1-24 (1971).
- [8] Generalized seniority states with definite isospin. Nucl. Phys. **A686**, 217-240 (2001).
- [9] Macchiavelli, A.O. *et al.*. Is there np pairing in  $N=Z$  nuclei? Phys. Rev. **C61**, 041303(R) (2000).
- [10] Afanasjev, A. & Frauendorf, S. Description of rotating  $N=Z$  nuclei in terms of isovector pairing. Phys. Rev. **C71**, 064318 (2005).
- [11] Danos, M. and Gillet, V. Stretch scheme, a shell model description of deformed nuclei. Phys. Rev. **161**, 10341044 (1967)
- [12] Marginean, N. *et al.*. Yrast isomers in  $^{95}\text{Ag}$ ,  $^{95}\text{Pd}$ , and  $^{94}\text{Pd}$ . Phys Rev. **C67**, 061301 (2003)
- [13] Alber, D., Bertschat, H. H., Grawe, H., Haas, H. & Spellmeyer, B. Nuclear structure studies of the neutron deficient  $N=50$  nucleus  $^{96}\text{Pd}$ . Z. Phys. **A332**, 129-135 (1989).
- [14] Schatz, H. *et al.*. End Point of the rp Process on Accreting Neutron Stars. Phys. Rev. Lett. **86**, 3471-3474 (2001).
- [15] Clement, R. R. C. *et al.* New approach for measuring properties of rp-process nuclei. Phys. Rev. Lett. **92**, 172502 (2004)
- [16] Scheurer, J. N. *et al.* Improvements in the in-beam  $\gamma$ -ray spectroscopy provided by an ancillary detector coupled to a Ge -spectrometer: the DIAMANT-EUROGAM II example. Nucl. Instrum. Methods Phys. Res. A **385**, 501510 (1997)
- [17] Gál, J. *et al.* The VXI electronics of the DIAMANT particle detector array. Nucl. Instrum. Methods Phys. Res. A **516**, 502510 (2004)
- [18] Skeppstedt, Ö. *et al.* The EUROBALL neutron wall design and performance tests of neutron detectors. Nucl. Instrum. Methods Phys. Res. A **421**, 531541 (1999)



- [19] Azaiez, F. EXOGAM: A  $\gamma$ -ray spectrometer for radioactive beams. Nucl. Phys. A 654, 1003c1008c (1999)
- [20] Simpson, J. et al. The EXOGAM array: a radioactive beam gamma-ray spectrometer. Heavy Ion Phys. 11, 159188 (2000); see also <http://pro.ganil-spiral2.eu/laboratory/detectors/exogam>
- [21] O'Leary, C.D. *et al.*. Neutron-proton pairing, Coulomb effects and shape coexistence in odd-odd N=Z  $^{46}\text{V}$ . Phys. Lett. B**459**, 73-80 (1999).
- [22] Lenzi, S.M. *et al.*. Band termination in the N=Z odd-odd nucleus  $^{46}\text{V}$  Phys. Rev. C **60**, 021303(R) (1999)
- [23] Heese, J. *et al.*. High spin states and shell model description of the neutron deficient nuclei  $^{90}\text{Ru}$  and  $^{91}\text{Ru}$ . Phys. Rev. C**49**, 1896-1903 (1994).
- [24] Marginean, N. *et al.*. Identification of excited states and shell model description of the N=Z+1 nucleus  $^{91}\text{Rh}$ . Phys. Rev. C**72**, 014302 (2005).

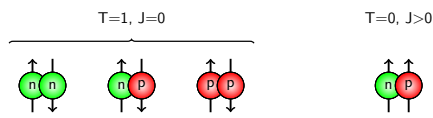


FIG. 1. Schematic illustration of the two possible pairing schemes in nuclei. The left part shows the normal isospin  $T = 1$  triplet. The two like-particle pairing components are responsible for most known effects of nuclear superfluidity. Within a given shell these isovector components are restricted to spin zero due to the Pauli Principle. The right part illustrates isoscalar  $T = 0$  neutron-proton pairing. Here the Pauli Principle allows only non-zero components of angular momentum.

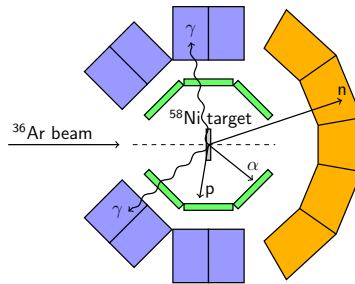


FIG. 2. Schematic illustration of the experimental set-up used to identify  $\gamma$ -ray transitions from excited states in  $^{92}\text{Pd}$ . The light particles and  $\gamma$ -rays emitted from the  $^{36}\text{Ar}+^{58}\text{Ni}$  reaction were observed using three different detector systems. The innermost detector array, DIAMANT[16, 17] (green), which consisted of 80 CsI scintillators, was used to detect light charged particles, mainly  $\alpha$ -particles and protons, and acted as a veto detector in the selection of events with no charged particles emitted. The Neutron Wall[18] (orange), comprising 50 liquid scintillator detectors and covering a solid angle of 1 in the forward direction, was used for the detection of evaporated neutrons. It is able to discriminate between neutron and  $\gamma$ -ray interactions by means of a combined time-of-flight and pulse-shape analysis technique. Gamma-rays emitted from the reaction products were detected using the EXOGAM[19, 20] high-purity Ge detector system (blue). Seven segmented Ge clover detectors were placed at an angle of  $90^\circ$  and four detectors at an angle of  $135^\circ$  relative to the beam direction, leaving room for the Neutron Wall at forward angles.

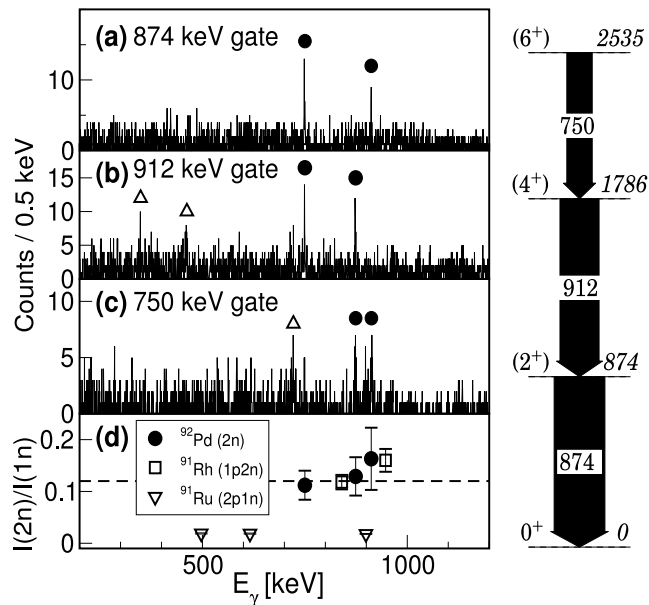


FIG. 3. **Left:** (a), (b), and (c) Gamma-ray energy spectra detected in coincidence with the 874 keV, 912 keV and 750 keV  $\gamma$  rays, with the additional requirement that two neutrons and no charged particle(s) were detected in coincidence. These  $\gamma$  rays correspond to transitions that we assign to depopulate the  $2^+$ ,  $4^+$  and  $6^+$  states in  $^{92}\text{Pd}$ , respectively and are marked by filled circles. Gamma rays from  $^{36}\text{Ar}$ -induced  $1p1n$ -evaporation reactions on small amounts of carbon deposited on the targets during irradiation, leading to  $^{46}\text{V}$  reactions are visible in b) and c) (open triangles). These  $\gamma$  rays appear in the projected spectra due to a combined effect of the limited detection efficiency for charged particles, the finite neutron/ $\gamma$  separation in the neutron detectors, the presence of  $\gamma$ -ray transitions at 914.9 keV and 750.7 keV in the level scheme of  $^{46}\text{V}$  [21, 22], and the fact that the reaction products from carbon contamination may recoil out of the target material, leading to Doppler broadening of such  $\gamma$  rays. **(d)** Intensity ratios of the  $\gamma$  rays assigned to  $^{92}\text{Pd}$  in coincidence with two neutrons and one neutron, respectively. The dashed line indicates the value expected for  $\gamma$  rays in coincidence with two neutrons, obtained from the 1n- and 2n-detection efficiencies. Measured intensity ratios for  $\gamma$  rays from previously known reaction products ( $^{91}\text{Ru}$  [23] and  $^{91}\text{Rh}$  [24]) are included for comparison. **Right:** Level scheme assigned to  $^{92}\text{Pd}$ . The energies (given in keV) and relative intensities (% , normalized to the intensity of the 874 keV transition) of the  $\gamma$ -ray transitions assigned to  $^{92}\text{Pd}$  are as follows: 873.6(2), 100(8); 912.4(2), 77(5); 749.8(3), 50(6). Given uncertainties are statistical.

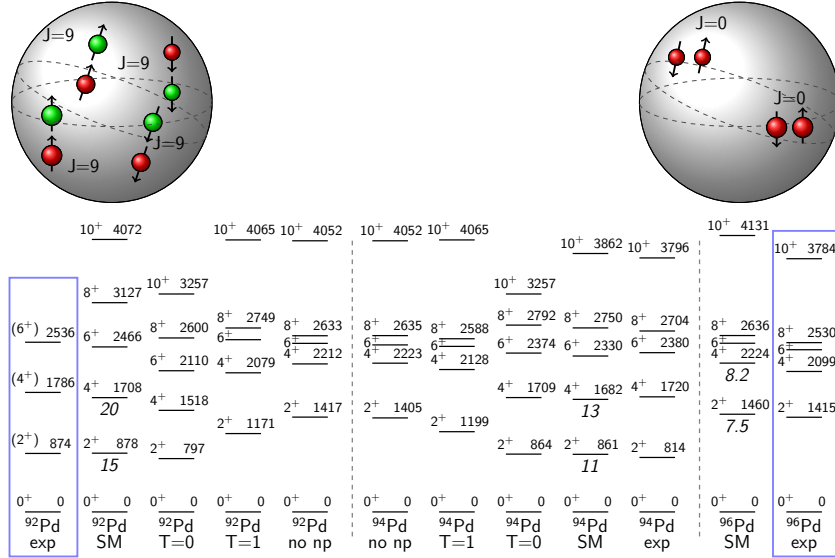


FIG. 4. **Lower panel:** Experimental level energies (keV) in the ground state bands of  $^{92}\text{Pd}$  (present work) and  $^{94,96}\text{Pd}$  [12, 13] compared with shell model predictions. Calculated  $B(E2 : 2^+ \rightarrow 0^+)$  and  $B(E2 : 4^+ \rightarrow 2^+)$  values (W.u.) are also shown in italic below the corresponding initial levels. The theoretical calculations for the spectra of  $^{92,94}\text{Pd}$  include, in addition to full neutron-proton interactions (SM), also results for pure  $T = 0$  and pure  $T = 1$  neutron-proton interactions. The results obtained without residual neutron-proton interactions (i.e. normal seniority coupling involving only isovector,  $T = 1$ , nn and pp pairing), are also shown for  $^{92,94}\text{Pd}$ .

**Top, left:** Schematic illustration of the structure of the ground-state wave function of  $^{92}\text{Pd}$  in the spin-aligned np paired phase. The main component of the wave function can be viewed as a system of deuteron-like np hole pairs with respect to the  $^{100}_{50}\text{Sn}_{50}$  “core”, spinning around the centre of the nucleus. **Top, right:** Schematic illustration of the structure of the ground-state wave function of  $^{96}\text{Pd}$  (normal pairing phase).